Sensory neuron targeting by self-complementary AAV8 via lumbar puncture for chronic pain

Benjamin Storek, Matthias Reinhardt, Cheng Wang, William G. M. Janssen, Nina M. Harder, Michaela S. Banck, John H. Morrison, and Andreas S. Beutler*

Departments of Medicine and Neuroscience, Mount Sinai School of Medicine, New York, NY 10029

Lumbar puncture (LP) is an attractive route to deliver drugs to the nervous system because it is a safe bedside procedure. Its use for gene therapy has been complicated by poor vector performance and failure to target neurons. Here we report highly effective gene transfer to the primary sensory neurons of the dorsal root ganglia (DRGs) with self-complementary recombinant adeno-associated virus serotype 8 (sc-rAAV8) modeling an LP. Transgene expression was selective for these neurons outlining their cell bodies in the DRGs and their axons projecting into the spinal cord. Immunohistochemical studies demonstrated transduction of cells positive for the nociceptive neuron marker vanilloid receptor subtype 1, the small peptidergic neuron markers substance P and calcitonin gene-related peptide, and the nonpeptidergic neuron marker griffonia simplicifolia isolectin B4. We tested the efficacy of the approach in a rat model of chronic neuropathic pain. A single administration of sc-rAAV8 expressing the analgesic gene prepro-β-endorphin (ppβEP) led to significant ($P < 0.0001$) reversal of mechanical allodynia for ≥ 3 months. The antiallodynic effect could be reversed by the μ-opioid antagonist naloxone 4 months after gene transfer ($P < 0.001$). Testing of an alternative nonopioid analgesic gene, IL-10, alone or in combination with ppβEP was equally effective ($P < 0.0001$). All aspects of the procedure, such as the use of an atraumatic injection technique, isotonic diluent, a low-infusion pressure, and a small injection volume, are consistent with clinical practice of intrathecal drug use. Therefore, gene transfer by LP may be suitable for developing gene therapy-based treatments for chronic pain.

adeno-associated virus | dorsal root ganglion | gene therapy | β-endorphin | IL-10

Chronic pain is common and often not relieved by available treatments. Opioid drugs, such as morphine, are the mainstay for the treatment of most severe pain states. Although their increased use has generally improved outcomes (1–4), opioid drugs fail in a significant number of patients (e.g., studies in cancer pain report failure rates of 12–66%) (5–8). Pure opioid agonists have no ceiling effect (9). However, associated toxicity is commonly dose-limiting. One strategy for reducing unwanted effects of a drug is to limit its site of action to regions that mediate the desired action and to avoid those that are problematic. Spinal opioid targeting by intrathecal (IT) administration is such a strategy. It is highly effective because μ-opioid receptors localized at the spinal level induce profound analgesia (10–13). The approach minimizes untoward effects by reducing the exposure of the brain and internal organs, where the CNS side effects (such as somnolence and hallucinations) and the peripheral side effects (such as refractory constipation) are mediated. In a clinical trial, IT opioids were superior to systemic opioids (14). However, IT opioid administration in patients requires the implantation of a pump and a permanent IT catheter, which has been associated with high complication rates (15–17), and is therefore, in practice limited to use by specialized medical teams at select centers.

Gene therapy holds considerable promise as a new treatment principle for nervous system disorders. Numerous therapeutic genes delivered by different vector systems have proven to be efficacious in pertinent animal models. A number of approaches have shown promise in clinical trials. At its core, the goal of nervous system gene therapy (i.e., *in vivo* gene transfer) is to improve upon traditional forms of drug delivery, e.g., reaching the brain side of the blood–brain barrier; providing a prolonged drug/gene effect; targeting drug/gene activity to a desired anatomical site; reducing side effects; and freeing patients from repeat injections, external pumps, and hazardous procedures. In addition, certain gene products may not have a conventional drug equivalent, e.g., certain larger proteins may not be available as a recombinant product or a small-molecule analogue, but can be encoded and delivered as a therapeutic gene in a vector.

To explore the potential of gene therapy for pain, we developed a therapeutic opioid gene for spinal delivery several years ago termed "prepro-β-endorphin" (ppβEP) (18), which showed analgesic efficacy for up to 2 weeks when expressed by an adenovirus but was shut down by immunity against the vector (19). Since then, new vector technology has become available for other applications. For instance, recombinant adeno-associated virus (rAAV) vectors were shown to mediate efficient *in vivo* gene transfer into nondividing cells, express transgenes in the long term, escape cellular immunity in most cases, and achieve reversal of pathology in various tissues, e.g., the retina. However, gene transfer by the IT route, i.e., by administration of vectors into the cerebrospinal fluid (CSF) by a lumbar puncture (LP) or other atraumatic technique, has remained challenging. Studies by other groups reported gene expression that was short-lived (20–23) unless vector administration was repeated, which extended expression to only 6 weeks (24); found that only meningeal fibroblasts could be transduced (19–21, 24) unless the vector was injected intraparenchymally (25–27); and/or relied on large-injection volumes, high-injection pressure, and hypertonic diluent (24, 28). In our own experience, we found various nonviral vector systems ineffective if administered IT (unpublished data), and we were similarly unable to detect transgene expression with conventional single-stranded rAAV serotype 2 (29). Therefore, we tested a variety of rAAV vector modifications, namely pseudotyping with capsids of different serotypes and the double-stranded, self-complementary rAAV (sc-rAAV).

Here we report that sc-rAAV serotype 8 (sc-rAAV8) very efficiently and selectively transduced the primary sensory neurons in the dorsal root ganglia (DRGs) if administered IT, established long-term gene expression after a single vector
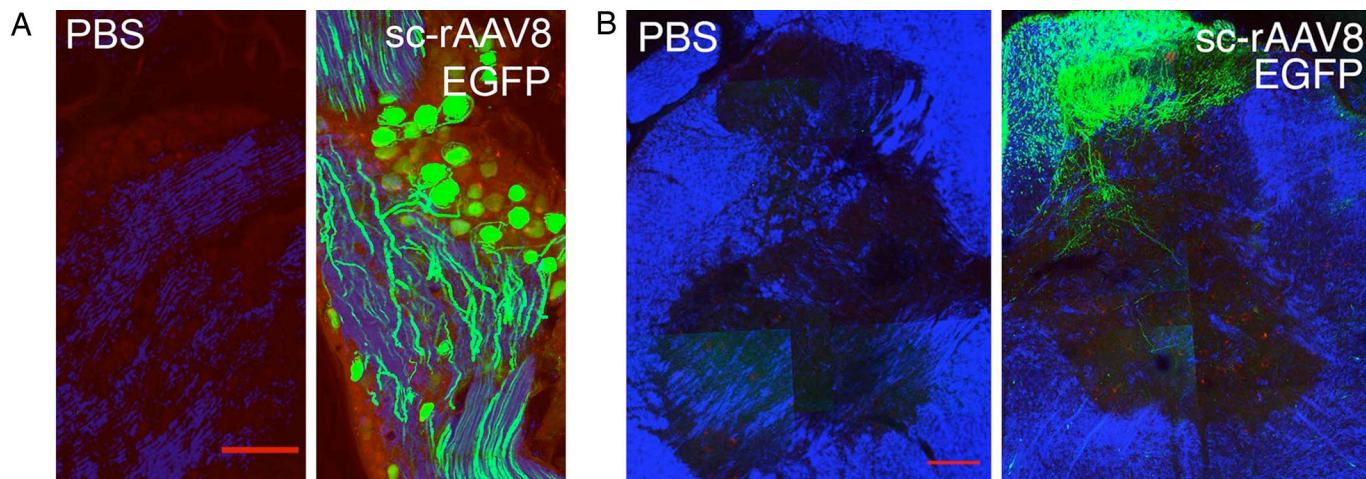
Fig. 1. Targeting of DRG neurons by IT sc-rAAV8. Neurons in lumbar DRGs and their axonal projections in the spinal cord showed specific fluorescence of the marker gene, EGFP, 1 month after vector administration (3×10^{10} sc-rAAV8 particles per animal). Nonneuronal cells in the DRG and cells intrinsic to the spinal cord were EGFP-negative. (*A*) (*Right*) Cells transduced in the DRG showed the typical morphology of primary sensory neurons with cell sizes up to 50 μm and occasional visualization of pseudounipolar axons. Axons and dendrites entering and exiting the DRG also were strongly EGFP-positive. (*Left*) No EGFP fluorescence was detected in sections from control DRGs. Because these tissue sections were unstained, the presence of comparable tissue in *Right* and *Left* was depicted by transmission light (blue) and unspecific fluorescence (red) outlining the DRG anatomy. To discriminate specific and unspecific fluorescence, the λ-stack mode was used on a Zeiss Meta 510 laser-imaging system (Carl Zeiss). Experimental and control tissues were prepared as blinded samples and imaged by using identical settings. (Scale bar: 200 μm.) (*B*) (*Right*) DRG neuron-derived axons entering the spinal cord as posterior nerve root were EGFP-positive. Fluorescent fibers can be traced penetrating into the posterior and midlayers of the gray matter and forming the fasciculus gracilis of the posterior white matter column. (*Left*) No EGFP fluorescence was present in the control tissue. Transmission light imaging (blue) delineates the gray and white matter. Unspecific fluorescence (red) was weak in spinal cord specimens. The sections shown are from the midlumbar level (approximately L5). (Scale bar: 200 μm.)

administration, and led to a significant reversal of allodynia in rats with neuropathic pain ($P < 0.0001$) for ≥ 3 months by expressing the analgesic gene ppβEP.

Results and Discussion

Targeting of DRG Neurons via the CSF. We modeled an LP in rats by atraumatic IT catheterization (30, 31) administering 3×10^{10} rAAV particles in 15 μl of isotonic PBS. All rAAV vectors in this study carried a short deletion in one inverted terminal repeat, which allows effective packaging of dsDNA genomes (32); expressed a single transgene under the control of the CMV promoter (32); and were pseudotyped with serotype 8 capsid (33), which was superior to serotype 1 [supporting information (SI) Fig. 5]. Serotype 1 is several-fold better than serotype 5 and markedly better than serotype 2, which fails in the IT space (29). sc-rAAV8-expressing EGFP (sc-rAAV8/EGFP) was used to identify gene-transfer targets. Microscopic examination of the brain, spinal cord, DRGs, nerve roots, and meningeal linings 1 month after gene transfer revealed strong specific EGFP fluorescence in DRG neurons and their axons and dendrites entering and exiting the DRG (Fig. 1*A*). Examination of the spinal cord showed EGFP fluorescence diagrammatically outlining the course of primary sensory neuron axons, which enter the spinal cord through the posterior nerve root, project into the posterior horn, and form the fasciculus gracilis of the posterior column (Fig. 1*B*). By using identical microscope settings, no EGFP-like fluorescence was detectable in control spinal cord tissue. In the brain, EGFP was undetectable by microscopy (data not shown) or Western analysis (SI Fig. 6*A*) and detectable at a level of only 10^{-4}-fold of DRGs by quantitative PCR (SI Fig. 6*B*).

Immunohistochemical (IHC) Characteristics of Transduced Neurons. Transduced cells were positive for the nociceptive neuron marker vanilloid receptor subtype 1 (TRPV1), the small peptidergic-neuron markers substance P (sP) and calcitonin gene-related peptide (CGRP), and the nonpeptidergic neuron marker griffonia simplicifolia isolectin B4 (IB4), as shown in Fig. 2.

Treatment of Chronic Pain in a Rat Neuropathy Model as Primary Study Endpoint. Chronic pain is one of the most common medical problems and a leading cause of disability. A frequent form of chronic pain is the neuropathic type, which is due to peripheral or central nerve injury caused by trauma, infection, metabolic disorders, cancer, drugs, or other etiologies. Available therapies frequently fail to control neuropathic pain, which has created considerable interest in new treatment strategies. Therefore, we tested whether sensory neuron gene therapy by IT sc-rAAV8 would be efficacious in neuropathic pain. We chose a widely accepted rat model, L5 spinal nerve ligation (SNL) (34). To test the analgesic potential of the vectors, we used two different known analgesic genes alone or in combination, one of which, ppβEP, we had previously developed (35). An 8-week pilot trial yielded strong preliminary evidence of efficacy (data not shown), established a reasonable pretest probability for a positive outcome of a subsequent study, and provided an estimate of effect size and variance for planning the definitive study presented here. The definitive study was blinded, randomized, and controlled; had a prospectively defined duration (i.e., 3 months from randomization) and primary endpoint (i.e., mechanical allodynia as assessed by von Frey testing of the paw-withdrawal threshold); and was analyzed with a statistical test, repeated-measures (0.5, 1, 2, and 3 months) ANOVA, that was corrected conservatively for multiple-group comparisons (Bonferroni method). In addition, we obtained a secondary endpoint, distress assessment of animals by a blinded observer, and performed additional statistical tests (e.g., Student's t test) for individual time points, which yielded confirmatory results.

Fig. 3 shows the withdrawal threshold of the ipsilateral (Fig. 3 *A* and *B*) and contralateral (Fig. 3 *C* and *D*) hind paw. The withdrawal threshold was ≥ 8.51 g at baseline. SNL resulted in a decrease of the ipsilateral withdrawal threshold in all rats to the allodynic range of <2.04 g. Sham-operated animals were not affected. The allodynic range was defined by the upper limit of the 95% C.I., i.e., ± 2 SD, of the withdrawal threshold of control animals over the full study period. Ten days after SNL (time
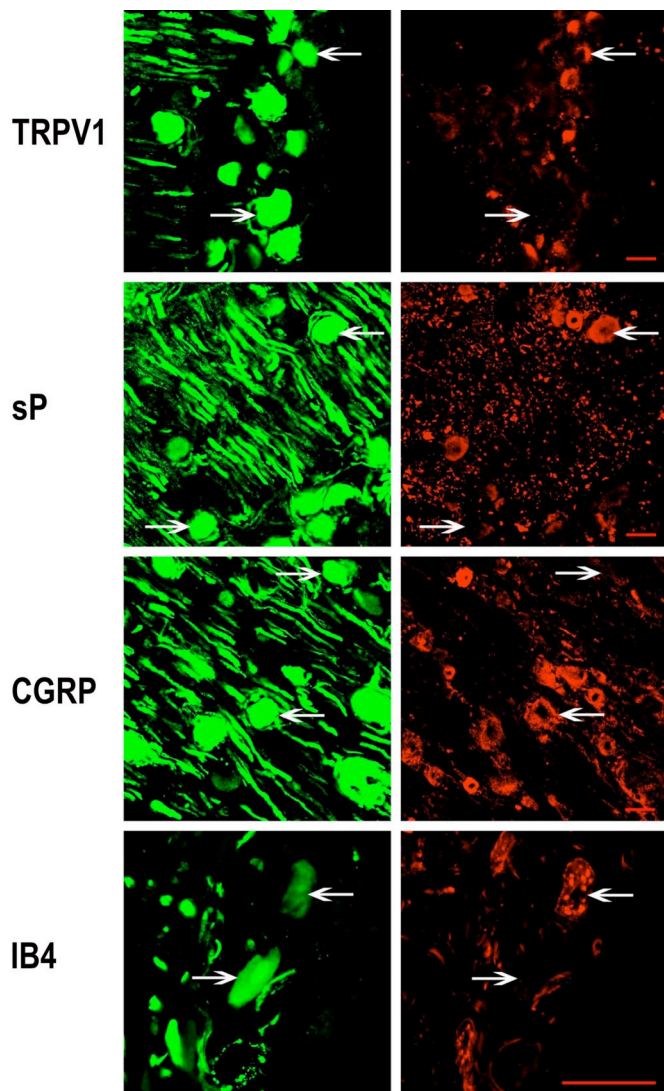
Storek *et al.*

Fig. 2. IHC characteristics of sc-rAAV8-transduced neurons. Laser-microscopic imaging in the two-channel/multitrack mode depicts EGFP expression (*Left*) (green; filter 505–530 nm) and staining with different IHC markers (*Right*) (red; filter 596–649 nm). sc-rAAV8 was found to transduce cells positive (left-pointing arrow) and negative (right-pointing arrow) for the nociceptive neuron marker TRPV1, for the small peptidergic neuron markers sP and CGRP, and for the nonpeptidergic neuron marker IB4. (Scale bars: 50 μm.)

point = 0), rats received IT therapeutic or control vectors or PBS by the blinded experimenter, who was provided with randomized coded tubes. Three groups received active treatment ($n = 12$ per group), namely sc-rAAV8 expressing ppβEP (sc-rAAV8/ppβEP, 3×10^{10} particles), or rat IL-10 (rIL-10) (discussed below; sc-rAAV8/rIL10, 3×10^{10} particles), or a half dose of sc-rAAV8/ppβEP (1.5×10^{10} particles) plus a half dose of sc-rAAV8/rIL10 (1.5×10^{10} particles). Two control groups received inactive injectate ($n = 7$), namely sc-rAAV8/EGFP (3×10^{10} particles) or PBS. Injectate (15 μl) was delivered through an IT catheter into the lumbar CSF (30, 31), as described for the marker gene studies above. From the time of IT vector injection at 0 months to the end at 3 months, the study was carried out in a strictly blinded fashion.

IT sc-rAAV8/ppβEP led to significant reversal of allodynia ($P < 0.0001$) as shown in Fig. 3*A*. The onset of therapeutic activity occurred between 0.5 and 1 month. In a subsequent

experiment determining the expression kinetic of IT sc-rAAV8/EGFP, we found that the onset of expression occurred between 0.5 and 1 month (Fig. 4). Therefore, we conclude that the delay in the onset of antiallodynic activity by sc-rAAV8/ppβEP is because of the gradual onset of transgene expression. The antiallodynic activity remained significant until the predefined end of the study at 3 months. There was a trend toward diminished activity between the 2- and 3-month time points. This trend was not significant and could have occurred by chance. Alternatively, it could be related to the development of tolerance to the opioid effect, although relative resistance of IT opioids to tolerization has been reported (36). Activity of sc-rAAV8/ppβEP persisted for at least 4 months, i.e., 1 month after the conclusion of this study, as implied by the naloxone-reversal experiment (Fig. 3*E*).

Efficacy of an Alternate Therapeutic Gene. In patients, the intensity of chronic pain typically varies over time, requiring adjustment of the analgesic dose or treatment regimen. Transgene expression by gene vectors can, in principle, be controlled by a regulated promoter, e.g., through the use of a tetracycline-responsive promoter. However, sc-rAAV vectors have a very limited packaging capacity, i.e., half of the typical maximum rAAV capacity of ≈4.8 kb, making it difficult to accommodate larger regulatory elements. For the clinical development of IT sc-rAAV8 for pain, two approaches could be considered. In the case of an opioid transgene such as ppβEP, the gene therapy would provide the baseline opioid dose, whereas additional opioids by mouth would be adjusted for worsening or break-through pain. Such a combination regimen would allow higher overall opioid doses with less severe side effects. Alternatively, one could consider the use of a transgene whose activity may not have a tight dose–response relationship. As an example, we chose rIL-10, which is believed to exert its known analgesic activity in neuropathic pain through the suppression of glial activation by its anti-inflammatory activity (35). Fig. 3*B* shows the antiallodynic effect of sc-rAAV8/rIL10. Allodynia resolved between 0.5 and 1 month after treatment paralleling the time course observed before. The therapeutic effect was significant when compared with the sc-rAAV8/EGFP or PBS control group ($P < 0.0001$) and remained stable until the conclusion of the study at 3 months. Use of rIL-10 for pain has been previously reported by others. However, the duration of activity in other reports has been <2 weeks for single administrations of vectors (20, 21) and up to 6 weeks only for a multiple-injection protocol using plasmid in hypertonic diluent (24). Our study demonstrates activity of IT rIL-10 in a pain model for as long as 3 months. In addition, we confirmed biochemically that rIL-10 was expressed 3.5 months after vector delivery (SI Fig. 7).

Clinical treatment protocols frequently combine several active treatments to increase efficacy or reduce side effects. We tested the efficacy of combining IT sc-rAAV8/ppβEP and sc-rAAV8/rIL10 each at half of the previously used dose such that the total dose of IT vector was the same as in the other groups. As seen in Fig. 3*B*, the combination had significant activity ($P < 0.0001$), but no more than either single vector at full dose. Although the activity may appear somewhat less than each single therapeutic vector at full dose, this finding was not statistically significant and is likely because of random variation. We conclude that the two vectors studied do not induce relevant synergy when combined and that their activity is additive, a common outcome when two treatments are combined.

Reversal of ppβEP Effect by μ-Opioid Blockade. The efficacy of opioids in the neuropathic variety of chronic pain is often questioned. ppβEP is an artificial gene (18, 19) designed to induce secretion of an opioid peptide, β-endorphin. To ascertain the mechanism of IT sc-rAAV8/ppβEP *in vivo*, we administered
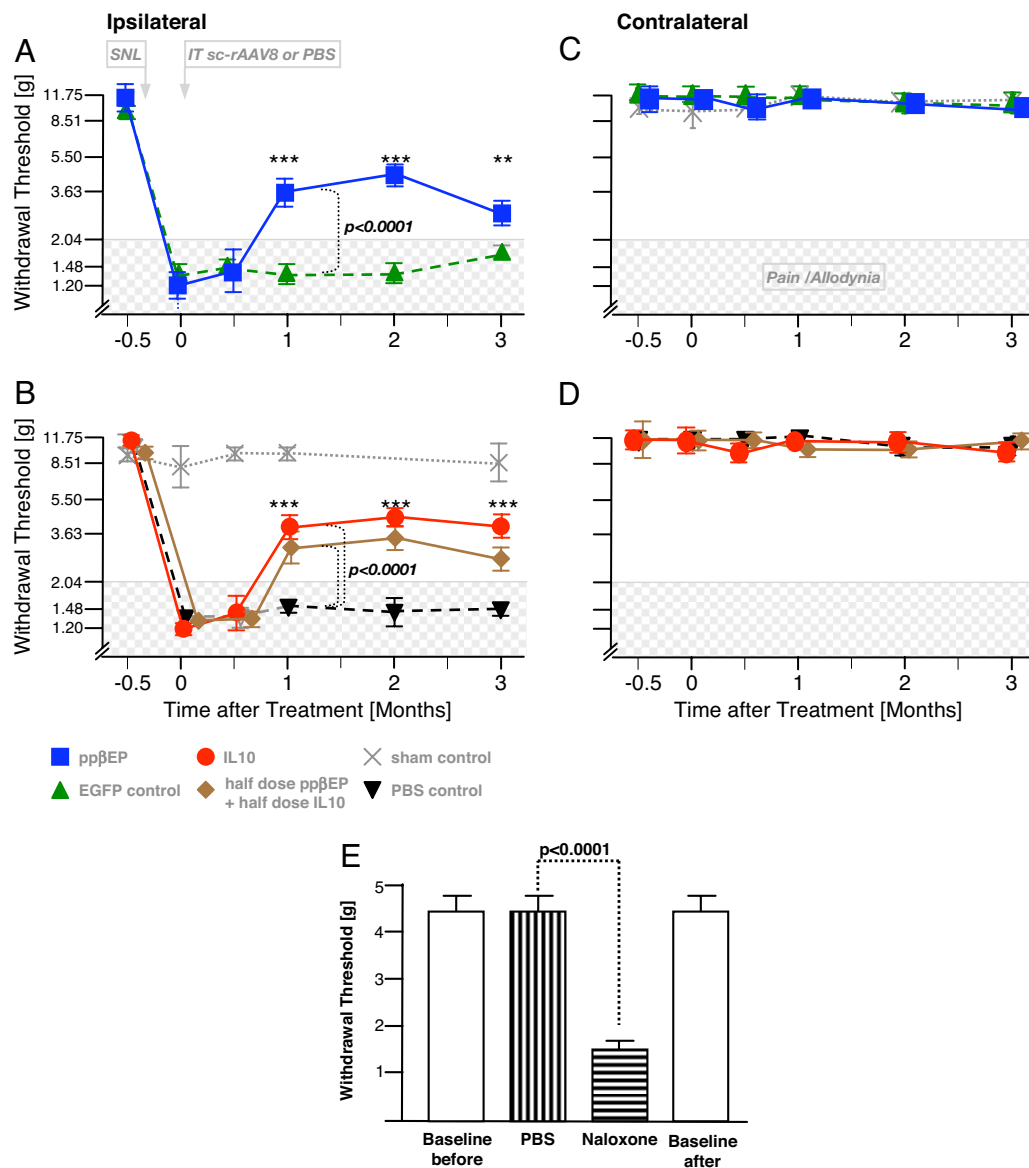
Fig. 3. Therapeutic efficacy of IT sc-rAAV8-expressing analgesic genes in a rat chronic neuropathic pain model. (*A–D*) Long-term alleviation of mechanical allodynia. Allodynia was assessed by paw-withdrawal threshold, which was ≥8.51 g in all animals at baseline (time point = −0.5 month) and in sham-operated controls (times signs) throughout. Paw-withdrawal threshold was quantified by using filaments of various stiffness measured in grams as indicated on the vertical axis (logarithmic scale; gradations correspond to the series of traditional Semmes Weinstein filaments used). SNL, which was performed 10 days before the start of the experiment, lowered the threshold to the allodynic range (≤2.04 g). IT sc-rAAV8 vectors or PBS were administered at time point 0. (*A*) IT sc-rAAV8 expressing the β-endorphin precursor gene ppβEP (filled squares) led to reversal of allodynia, which was significant ($P < 0.0001$) when compared with the sc-rAAV8/EGFP or PBS control group. The therapeutic effect became apparent between 0.5 and 1 month after vector administration, reflecting the gradual onset of transgene expression by IT sc-rAAV8, and lasted until the end of the experiment at 3 months. Vectors expressing the biologically inert marker gene EGFP had no effect (filled triangles). (*B*) rIL-10 expression by IT sc-rAAV8/rIL10 (filled circles) had a similar therapeutic effect, which also was statistically significant ($P < 0.0001$). A combination of vectors expressing ppβEP and rIL-10 (filled diamonds) each administered at half dose (resulting in the same total vector dose as in the other groups) also was effective ($P < 0.0001$, compared with controls) but was not statistically different from administering one of the active viruses at full dose ($P = 1$, compared with IL-10; $P = 0.08$, compared with ppβEP). IT PBS (filled inverted triangles) had no effect and was not different from sc-rAAV8/EGFP ($P = 1$). (*C* and *D*) None of the IT vectors affected the withdrawal threshold of the contralateral hind paw, suggesting that there was no direct effect on the motor system. The experimenter was blinded to group assignment. Group sizes were as follows: sc-rAAV8/ppβEP, $n = 9$; sc-rAAV8/rIL10, $n = 12$; sc-rAAV8/ppβEP (half dose) plus sc-rAAV8/rIL10 (half dose), $n = 10$; sc-rAAV8/EGFP, $n = 7$; PBS, $n = 6$; sham, $n = 4$. All animals received a total dose of 3×10^{10} vector particles in an injectate volume of 15 μl through an IT catheter into the lumbar CSF. Six animals were excluded from the study within 1 h of vector injection because of IT bleeding or neurological deficits upon recovery from anesthesia, resulting in unequal group sizes by chance, which could not be compensated for because the experimenter was blinded. For the remaining 44 animals, data collection was complete until the experimenter was unblinded at the prospectively defined study endpoint at 3 months. Shown is the median ± SEM. Statistical testing for differences between groups was performed by a repeated-measures (0.5, 1, 2, and 3 months) ANOVA, with Bonferroni adjustment for multiple-group comparisons (division by 10 for 10 possible comparisons among five groups). *P* values indicated in the graph ($P < 0.0001$) are the comparisons between the treatment and control groups taken from this analysis. As a secondary analysis, a *t* test was performed for individual time points, which also yielded significant results as indicated in the graph. ∗∗∗, $P < 0.001$; ∗∗, $P < 0.01$. (*E*) μ-Opioid receptor mechanism of sc-rAAV8/ppβEP. One month after conclusion of the main study, sc-rAAV8/ppβEP-treated animals were subjected to a follow-up experiment testing whether persisting analgesic activity could be reversed by the μ-opioid receptor antagonist naloxone. Baseline paw-withdrawal threshold was assessed on days 1 and 4. Animals were randomized to receive 0.3 mg/kg naloxone on day 2 or 3. On the alternate day, the vehicle control (PBS) was given. Naloxone induced a reversal of the allodynic state, whereas PBS had no effect ($P < 0.001$). The experimenter was blinded to drug assignment.
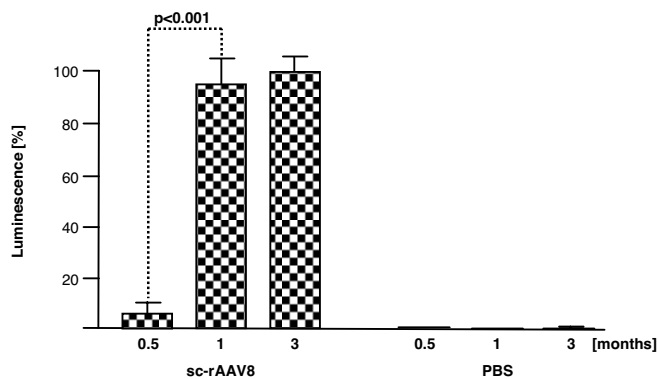
Fig. 4. Kinetics of IT sc-rAAV8/EGFP gene expression. EGFP in the lumbar part of the spinal cord (homogenized with all nerve roots and DRGs attached) was quantified by Western blotting at three time points. Expression was minimal at 0.5 month after vector administration, rose significantly until 1 month, and then remained unchanged until 3 months. Shown is the mean ± SEM of detected luminescence standardized to the highest mean (set to 100%). Group sizes were as follows: 0.5- and 1-month groups, $n = 6$; 3-month group, $n = 11$. Luminescence in tissue from PBS-injected rats represents the unspecific background level.

the μ-opioid receptor antagonist naloxone and found that it induced a temporary relapse of marked allodynia, whereas PBS had no effect (Fig. 3E). This experiment was performed in the sc-rAAV8/ppβEP-treated animals 1 month after the conclusion of the main study, i.e., 4 months after IT vector administration. To ensure an objective assessment of the naloxone effect, the experimenter was blinded to the random assignment to naloxone versus PBS.

Secondary Endpoints. In human analgesic studies, pain is usually not measured by behavior tests but by recording patients' subjective assessment of comfort. This approach was recently extended to the evaluation of analgesics in animals, e.g., a study using companion dogs reported subjective assessment of the animal's pain state by its owners as an endpoint (37). We added a similar approach as a secondary endpoint, namely a subjective aggregate assessment by the blinded experimenter of whether individual animals appeared to be comfortable or displayed pain behavior throughout the study period. We recorded the results on a three-tiered scale as pain behavior present, indeterminate, or absent. As shown in Table 1, the majority of sc-rAAV8/ppβEP-, sc-rAAV8/rIL10-, and combination-treated animals appeared comfortable, whereas the majority of control group animals appeared to be in pain. We regard this part of the assessment only as a secondary endpoint because such methods have not been validated yet in rodents, but we suggest that it may be meaningful because results were clearly not random ($P <$ 0.0001 in a χ^2 test of association).

One could argue that an unrecognized vector-induced alteration of DRG cells led to the observed reversal of allodynia. However, several observations would be inconsistent with this

Table 1. Clinical pain behavior

Vector	+	+/−	−
rIL-10	0	2	10
ppβEP	0	2	7
rIL10 plus ppβEP	0	3	7
EGFP	5	2	0
PBS	6	0	0

+, pain behavior present; +/−, pain behavior indeterminate; −, pain behavior absent.

notion. First, vectors expressing EGFP had no effect compared with PBS, suggesting that toxicity would have to be related to the transgene. Second, comparable therapeutic efficacy was achieved with two structurally unrelated genes, making it increasingly unlikely that both would be similarly toxic. Third, naloxone-induced reversal of allodynia could be demonstrated 4 months after vector administration, showing that the neural mechanisms mediating the allodynic behavior response remained intact throughout the entire study period and could be unmasked. Taken together, these findings support the conclusion that the lasting reversal of allodynia observed was because of a bona fide therapeutic gene effect persisting throughout the study period.

The onset of the antiallodynic effect was delayed, occurring after 0.5 month. As demonstrated in Fig. 4, this kinetic tracks the onset of transgene expression, which occurs slowly in most rAAV applications.

Conclusions. The present study demonstrated highly efficient and selective gene transfer into primary sensory neurons by administration of sc-rAAV8 vectors into the lumbar CSF. Transduction was selective for DRG neurons and did not affect other cells of the CNS. Several IHC-distinct classes of DRG neurons were transduced. At the center of our study was the demonstration of efficacy in a chronic neuropathic pain model, an important functional outcome. Unlike previous reports, the observed efficacy was long term, lasting for at least 3 months after a single administration of vectors. The injection technique was atraumatic, modeling an LP and thereby circumventing requirements for injections at multiple sites or for intraparenchymal injections into CNS tissue. Furthermore, we administered the vector in a small volume of isotonic injectate, which is comparable to the volume and diluent of currently approved conventional IT drugs.

Other studies attempting gene transfer by LP failed to transduce neural tissue (19–21, 24); resulted in transgene expression for <2 weeks (20–23); required multiple injections (extending expression to <6 weeks) (24); used hypertonic diluent (24); used high electrical currents *in vivo* (22, 23); injected intraparenchymally instead of into the CSF (25–27); and/or infused large volumes (28). Such approaches may not be good candidates for clinical trials because of safety concerns. For instance, in one study, 100 μl of the vector solution was infused IT into 20-g mice (28), which would correspond to >500 ml in a human, a prohibitive volume for LP administration. Our study administered IT vector in 15 μl of isotonic diluent to adult rats weighing ≥300 g, which corresponds to 4.5 ml in patients when calculations are performed on the basis of bodyweight and less on the basis of body surface area, i.e., an FDA-approved volume for currently used IT drugs. Although any new drug approval is only limited by an individual risk–benefit analysis, it would appear helpful in the case of IT gene therapy if the vector requirements would not lie far outside of the parameters, for which clinical experience exists, e.g., hypertonic diluent would likely raise concern because it would be expected to cause brain edema. HSV has been proposed for pain gene therapy by injection into the limbs (38, 39). Its peculiar route of administration follows the unique biology of the vector (uptake by peripheral nerves) and requires multiple injections into the skin or other peripheral tissue sites. HSV vectors also may be inflammatory in humans because of retained wild-type genes.

The approach to IT gene transfer for pain presented here requires only a single standardized injection feasible in patients by LP (in this study, modeled in rats by atraumatic catheterization); confers long-term efficacy; accommodates different therapeutic genes; and uses a noninflammatory vector with a unique safety record, rAAV, from which all viral genes have been removed and whose parent wild-type virus has never been associated with a clinical disease. Our observations in rodents

raise the possibility that sc-rAAV8 by LP may be a candidate for developing clinically viable strategies for sensory neuron gene therapy for pain. Additional studies are required to assess the possibility of long-term toxicity from the vector or gene product in rodents and large animals. Ultimately, the approach could be clinically tested for safety and efficacy in patients with an underlying advanced disease (like incurable cancer), who have a high prevalence of neuropathic pain and an unmet need for improved symptom control (40).

Experimental Procedures and Methods

Statistical Methods. Groups retested at several time points (Fig. 3A) were compared with a repeat-measures ANOVA by using the software SAS 9.1 (SAS Institute), with adjustment for multiple comparisons by the Bonferroni method. The clinical pain behavior outcome, a secondary endpoint (Table 1), was treated as a contingency table, and the overall significance of the observed effect was determined by the χ^2 test of association by using the inferential statistics tools available online through Vassar College (http://faculty.vassar.edu/lowry/newcs.html). To compare the effect of naloxone and PBS (Fig. 3E) and to assess the effect of IT therapy at individual time points, a secondary endpoint, Student's two-sided t test was performed by using the software JMP 6.02 (SAS Institute).

Vector Design. sc-rAAV vectors were produced in our laboratory by triple-plasmid transfection, followed by several rounds of cesium chloride gradient purification, dialysis, and concentration. The proviral vector genome encoding the sc-AAV genome was a generous gift from D. McCarty (Children's Research Institute, Columbus, OH) (32). The construct expresses EGFP under the control of the CMV promoter. EGFP was replaced by the ppβEP transgene (previously reported in ref. 18) or by rIL-10 cDNA (requested from the authors of ref. 24) by standard subcloning procedures, leaving the CMV promoter intact. The packaging plasmid, a generous gift from J. Wilson (University of Pennsylvania, Philadelphia, PA) (33), encoded the serotype 8 capsid protein.

Animals, Vector Delivery, and Behavior Testing to Assess Allodynia. Procedures were approved by the Institutional Animal Care and Use Committee. Male Harlan Sprague–Dawley rats with masses of ≈350 g were subjected to SNL (34). Briefly, under anesthesia, the spinal nerve injury was produced by ligating and transecting the right L5 spinal nerve distal to the L5 DRG. After incision of the skin, the right paraspinal muscles were separated from the spinous processes at the L5–S1 levels. The right L6 transverse process was resected with a small rongeur to visualize the L4 and L5 spinal nerves. The L5 spinal nerve was isolated, tightly ligated, and transected. In sham-operated control animals, the right L5 spinal nerve was exposed as described, but not ligated or transected. The paraspinal muscles were approximated with surgical sutures, and the skin was closed with 9-mm wound clips. The IT catheterization was performed as described by Yaksh (30, 31). Briefly, under gaseous anesthesia, the atlanto-occipital membrane was exposed, and a 2-mm-long incision was made, cutting the dura and arachnoid membrane. A 9-cm-long prestretched PE10 polyethylene tube catheter was inserted through the cisterna magna into the IT space and advanced to the caudal end of the spinal cord; 3×10^{10} viral particles suspended in 15 μl of PBS were injected over 1 min. After withdrawal of the catheter, the neck muscles were approximated with surgical sutures, and the skin was closed with 9-mm wound clips.

Mechanical allodynia was quantified with the von Frey test (41), our primary endpoint (Fig. 3). In addition, we used observation of clinical pain behavior as a secondary endpoint (Table 1). Briefly, rats were placed on a wire mesh, allowing access to the paws. Spontaneous rat behavior was observed, with special attention to standing postures, walking, and resting position. Graded von Frey filaments (Stoelting) were applied at the midplantar area of the right and left hind paws and depressed slowly until they bent. The filaments were tested in order of increasing logarithmic stiffness (0.41, 0.69, 1.2, 1.48, 2.04, 3.63, 5.5, 8.51, 11.75, and 15.14 g), with each applied three times. The first filament in the series that evoked three reflexive withdrawals from the three applications was designated the threshold.

IHC and Imaging. Tissue preparation and imaging were performed by using standard IHC techniques and microscopic examination on a Zeiss 510 Meta confocal scanning microscope (Carl Zeiss). Details are provided in *SI Text*.

Western Blotting. Western blotting for EGFP was performed with the antibody JL-8 (BD Biosciences). Chemiluminescence was detected with the LAS-3000 cooled-camera system (Fuji). Data were exported in tiff format and quantified with the Image J densitometry software (National Institutes of Health).

1. World Health Organization (1986) *Cancer Pain Relief* (WHO, Geneva).
2. Portenoy RK (1995) *Semin Oncol* 22:112–120.
3. Levy MH (1996) *N Engl J Med* 335:1124–1132.
4. Jacox A, Carr D, Payne R (1994) in *Clinical Practice Guideline Number* 9 (Agency for Health Care Policy and Research, U.S. Department of Health and Human Services, Public Health Service, Rockville, MD), AHCPR publication 94-0592.
5. Zech DF, Grond S, Lynch J, Hertel D, Lehmann KA (1995) *Pain* 63:65–76.
6. Caraceni A, Portenoy RK (1999) *Pain* 82:263–274.
7. Meuser T, Pietruck C, Radbruch L, Stute P, Lehmann KA, Grond S (2001) *Pain* 93:247–257.
8. Weiss SC, Emanuel LL, Fairclough DL, Emanuel EJ (2001) *Lancet* 357:1311–1315.
9. Pasternak GW (1993) *Clin Neuropharmacol* 16:1–18.
10. Yaksh TL, Rudy TA (1976) *Science* 192:1357–1358.
11. Mansour A, Fox CA, Burke S, Akil H, Watson SJ (1995) *J Chem Neuroanat* 8:283–305.
12. Minami M, Maekawa K, Yabuuchi K, Satoh M (1995) *Brain Res Mol Brain Res* 30:203–210.
13. Bunzow JR, Zhang G, Bouvier C, Saez C, Ronnekleiv OK, Kelly MJ, Grandy DK (1995) *J Neurochem* 64:14–24.
14. Smith TJ, Staats PS, Deer T, Stearns LJ, Rauck RL, Boortz-Marx RL, Buchser E, Catala E, Bryce DA, Coyne PJ, Pool GE (2002) *J Clin Oncol* 20:4040–4049.
15. Crul BJ, Delhaas EM (1991) *Reg Anesth* 16:209–213.
16. Devulder J, Ghys L, Dhondt W, Rolly G (1994) *J Pain Symptom Manage* 9:75–81.
17. Mercadante S (1999) *Cancer* 85:1849–1858.
18. Beutler AS, Banck MS, Bach FW, Gage FH, Porreca F, Bilsky EJ, Yaksh TL (1995) *J Neurochem* 64:475–481.
19. Finegold AA, Mannes AJ, Iadarola MJ (1999) *Hum Gene Ther* 10:1251–1257.
20. Milligan ED, Langer SJ, Sloane EM, He L, Wieseler-Frank J, O'Connor K, Martin D, Forsayeth JR, Maier SF, Johnson K, *et al.* (2005) *Eur J Neurosci* 21:2136–2148.
21. Milligan ED, Sloane EM, Langer SJ, Cruz PE, Chacur M, Spataro L, Wieseler-Frank J, Hammack SE, Maier SF, Flotte TR, *et al.* (2005) *Mol Pain* 1:9.
22. Lin CR, Tai MH, Cheng JT, Chou AK, Wang JJ, Tan PH, Marsala M, Yang LC (2002) *Neurosci Lett* 317:1–4.
23. Lin CR, Yang LC, Lee TH, Lee CT, Huang HT, Sun WZ, Cheng JT (2002) *Gene Ther* 9:1247–1253.
24. Milligan ED, Sloane EM, Langer SJ, Hughes TS, Jekich BM, Frank MG, Mahoney JH, Levkoff LH, Maier SF, Cruz PE, *et al.* (2006) *Pain* 126:294–308.
25. Eaton MJ, Blits B, Ruitenberg MJ, Verhaagen J, Oudega M (2002) *Gene Ther* 9:1387–1395.
26. Xu Y, Gu Y, Wu P, Li GW, Huang LY (2003) *Hum Gene Ther* 14:897–906.
27. Xu Y, Gu Y, Xu GY, Wu P, Li GW, Huang LY (2003) *Proc Natl Acad Sci USA* 100:6204–6209.
28. Watson G, Bastacky J, Belichenko P, Buddhikot M, Jungles S, Vellard M, Mobley WC, Kakkis E (2006) *Gene Ther* 13:917–925.
29. Storek B, Harder NM, Banck MS, Wang C, McCarty DM, Janssen WG, Morrison JH, Walsh CE, Beutler AS (2006) *Mol Pain* 2:4.
30. Yaksh TL, Rudy TA (1976) *Physiol Behav* 17:1031–1036.
31. Malkmus SA, Yaksh TL (2004) *Methods Mol Med* 99:109–121.
32. McCarty DM, Fu H, Monahan PE, Toulson CE, Naik P, Samulski RJ (2003) *Gene Ther* 10:2112–2118.
33. Gao GP, Alvira MR, Wang L, Calcedo R, Johnston J, Wilson JM (2002) *Proc Natl Acad Sci USA* 99:11854–11859.
34. Chung JM, Kim HK, Chung K (2004) *Methods Mol Med* 99:35–45.
35. Beutler AS, Banck MS, Walsh CE, Milligan ED (2005) *Curr Opin Mol Ther* 7:431–439.
36. Roerig SC, O'Brien SM, Fujimoto JM, Wilcox GL (1984) *Brain Res* 308:360–363.
37. Brown DC, Iadarola MJ, Perkowski SZ, Erin H, Shofer F, Laszlo KJ, Olah Z, Mannes AJ (2005) *Anesthesiology* 103:1052–1059.
38. Glorioso JC, Fink DJ (2002) *Curr Opin Drug Discov Dev* 5:289–295.
39. Mata M, Glorioso JC, Fink DJ (2004) *Curr Neurol Neurosci Rep* 4:1–2.
40. Manfredi PL, Gonzales GR, Sady R, Chandler S, Payne R (2003) *J Palliat Care* 19:115–118.
41. Chaplan SR, Bach FW, Pogrel JW, Chung JM, Yaksh TL (1994) *J Neurosci Methods* 53:55–63.

SI Figures and Text for

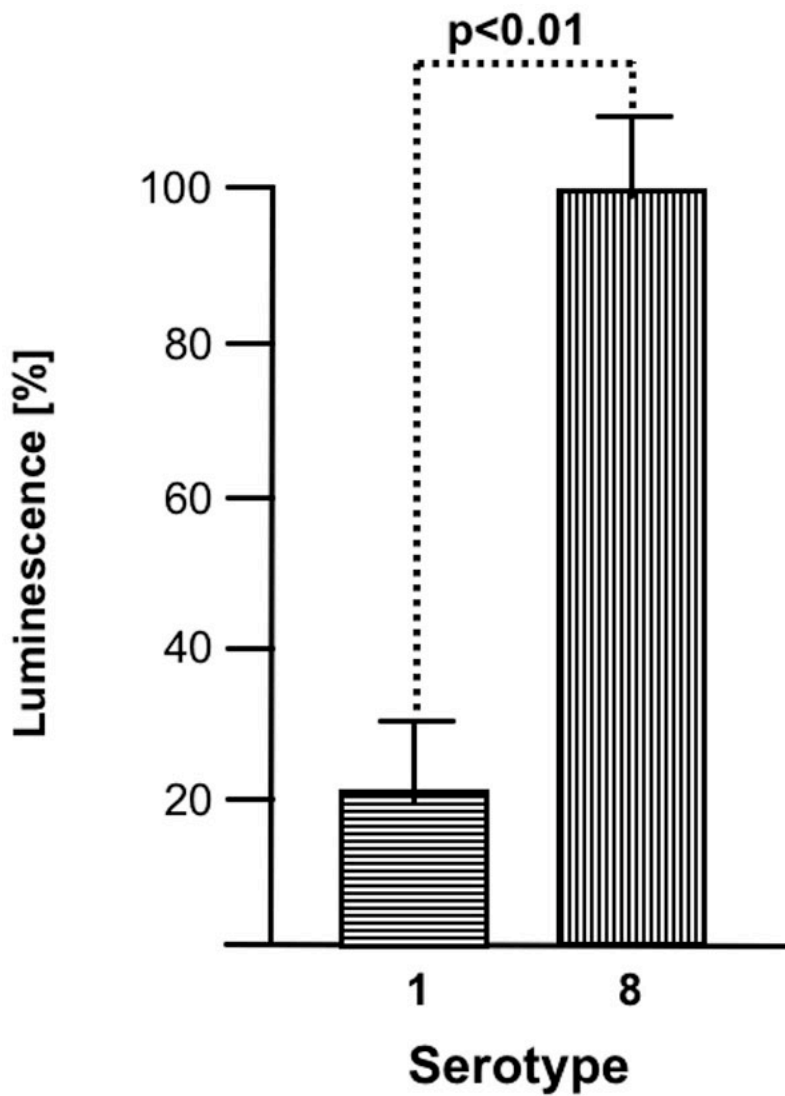## Storek et al., PNAS, 22 (105/3): 1055-60, 2008.

Fig. 5. Choice of serotype 8 capsid. sc-rAAV vectors pseudotyped with serotype 8 capsids showed superior expression in the IT gene-transfer paradigm used. Rats were injected with IT sc-rAAV ($3\times$ 10^9 vector genomes per animal) as described. After 1 month, the lumbosacral spinal cord was harvested with the meninges and DRGs attached and EGFP expression quantified (methods as described for Fig. 4). Shown here is the mean $\pm$ SEM of the luminescence for each group ($n = 4$). (Of note, for this figure, the background luminescence, i.e., luminescence of the membrane in an empty lane, was subtracted as for Fig. 4, but unlike SI Fig.6).
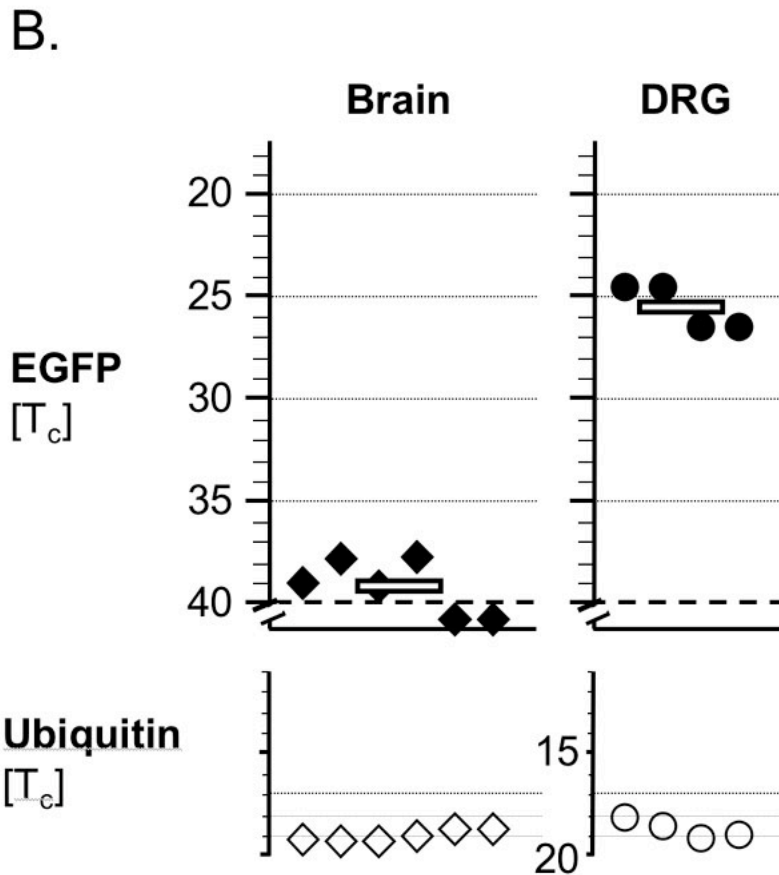
A.
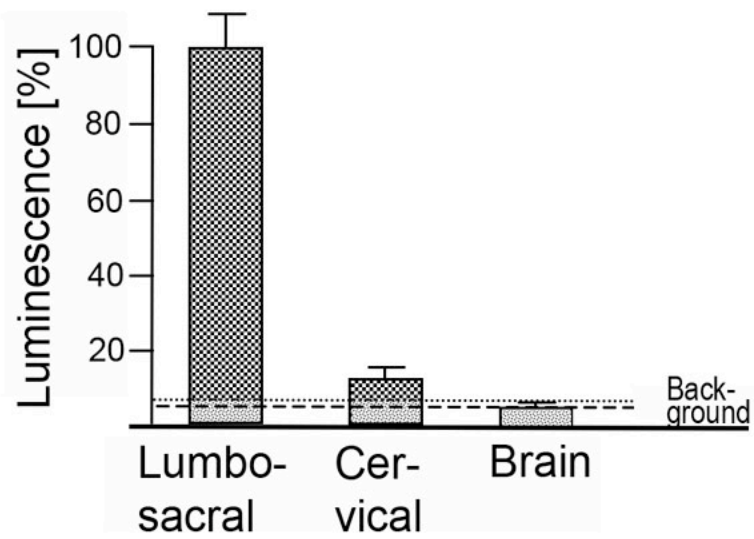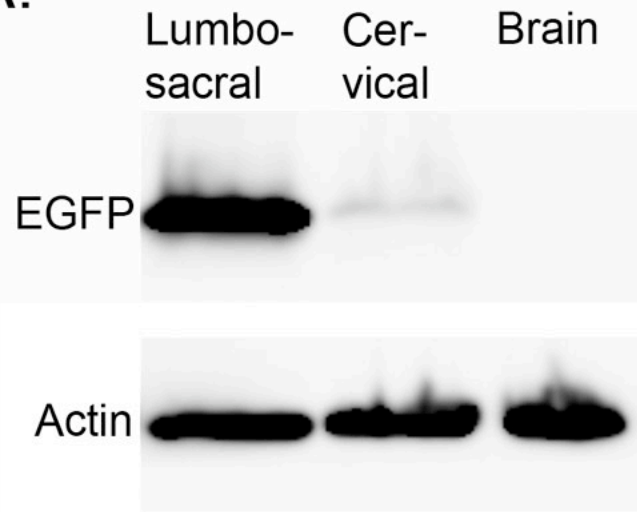
Fig. 6. Transgene product detection in the brain. (*A*) Western analysis of whole-brain homogenates from animals injected IT with sc-rAAV8/EGFP (3×10^{10} vector genomes per animal) 1 month prior demonstrated no detectable EGFP protein. (*Upper*) A blot from a single animal along with an actin loading control is shown. (*Lower*) In addition, the bar graph depicts the mean± SEM of the luminescence for each group of animals ($n = 4$). Chemiluminescence was detected directly by exposure of the membrane in a cooled-camera system and is shown without prior background subtraction. Mean background luminescence (horizontal broken line) and the upper limit of the 95% C.I. of the background luminescence (horizontal dotted line) were calculated from equal-sized control areas. The mean luminescence of brain samples was below the background level as shown. The difference between the lumbosacral and cervical portions of the spinal cord is because of the inclusion of the cauda equina in the lumbosacral tissue sample, which encompasses the sensory nerve roots containing substantial amounts of EGFP produced by lumbar DRG neurons. (*B*) Expression of EGFP was detectable in only four of six brains ($T_c < 40$ cycles) from IT sc-rAAV8/EGFP-injected animals ($3 ´ 10^{10}$ vector genomes per animal) when assessed by quantitative PCR. The median difference compared with lumbar DRGs ($n = 4$) was 13.4 cycles, corresponding to a $>10^4$-fold difference (quantitative PCR efficiency of >95%). Shown are the threshold cycles (T_c) for each sample measured and the median for each group. The difference between the groups was significant ($P < 10^{-6}$).
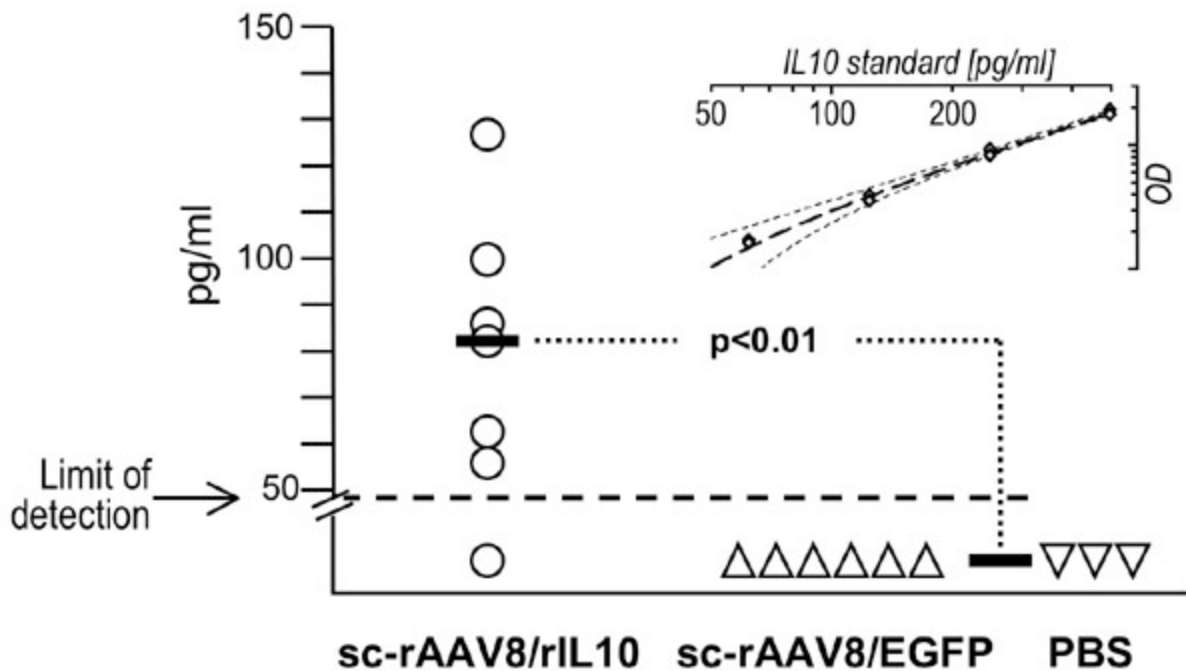
Fig. 7. Biochemical detection (ELISA) of the therapeutic transgene product. rIL-10 was detectable by ELISA in the CSF of rats 3.5 months after IT injection of sc-rAAV8/rIL10 (six of seven samples were positive) and not in CSF of sc-rAAV8/EGFP or PBS controls (zero of six samples and zero of three samples, respectively). The median concentration in the experimental group was 83 pg/ml, and the median of the controls was undetectable. Results for individual rats are shown (circles, sc-rAAV8/rIL10; triangles, sc-rAAV8/EGFP; inverted triangles, PBS; horizontal bars, median of experimental and control samples). The limit of detection was 48 pg/ml (broken horizontal line), which was determined by the upper 95% C.I. of OD obtained of independent negative standards ($n = 16$). (*Inset*) Test characteristics (broken line, standard curve; dotted line, 95% C.I. around standard curve). To estimate the significance level, the number of samples with detectable rIL-10 levels was compared between the experimental group and the controls by using the χ^2 test as described in *Experimental Procedures and Methods* (χ^2 test statistical analysis as used for Table 1). Reagents were purchased as Quantikine rat IL-10 Immunoassay Kit (catalog no. R1000; R&D Systems) and used according to the manufacturer's instructions.

SI Experimental Procedures and Methods

Tissue Preparation and IHC. Rats were transcardially perfused with 1% paraformaldehyde in PBS for 1 min, followed by 4% paraformaldehyde PBS for 12 min. Spinal cord and DRGs were completely excised and postfixed in 4% paraformaldehyde PBS for 24 h. Tissue was cryoprotected, frozen, cut with a cryostat (Reichert-Jung) at a slice thickness of 15μm, and dried overnight. For IHC tissue, sections were permeabilized with 0.5% Triton X-100 in PBS for 1 h and blocked with 10% normal goat serum/0.1% gelatin in PBS (with 0.05% Triton X-100) for 2 h. Slides were subsequently stained with biotinylated IB4 (Sigma-Aldrich) and were additionally blocked with a biotin-avidin blocking kit (Vector Laboratories). Antibody dilutions were as follows: TRPV1, 1:1,000 (Affinity BioReagents); CGRP, 1:1,000 (Sigma-Aldrich); substance P, 1:1,000 (ImmunoStar); IB4, 10μg /ml; and neurotrace deep red, 1:300 (Molecular Probes). Sections were incubated with the primary antibodies for 48 h at

4°C. A secondary antibody, an Alexa Fluor 594-labeled goat anti-rabbit antibody, was used at a dilution of 1:200 (Invitrogen). Biotinylated IB4 was visualized with a Texas Red-labeled Avidin D used at a concentration of 1:200 (Vector Laboratories). All slides were cover-slipped with PermaFluor-mounting medium (Thermo Electron).

Microscopy. Imaging was performed on a Zeiss 510 Meta confocal microscope by using a 488-nm excitation. For Fig. 1, the λ-stack method was used to differentiate specific EGFP fluorescence from unspecific background. Anatomical landmarks were imaged with transmission light. Overlay images were prepared showing EGFP green, unspecific background red, and transmission light imaging blue. Panels in Fig. 1*B* were montaged from several images to accommodate the limited anatomic coverage of the ✕10 objective. For Fig. 2, the two-channel, multitrack mode was used with 488-nm excitation/505-530-nm filter for EGFP and 543-nm excitation/596-649-nm filter for Alexa Fluor 594 or Texas Red.